

# Complex Pattern Formation in the Polyacrylamide–Methylene Blue–Oxygen Reaction

Oliver Steinbock,<sup>\*,†</sup> Eric Kasper,<sup>‡</sup> and Stefan C. Müller<sup>‡</sup>

Department of Chemistry, Florida State University, Tallahassee, Florida 32306-4390, and  
Institut für Experimentelle Physik, Otto-von-Guericke-Universität Magdeburg, Universitätsplatz 2,  
D-39106 Magdeburg, Germany

Received: February 23, 1999

The polyacrylamide–methylene blue–oxygen system reveals a variety of complex concentration patterns. Chevron and white-eye patterns develop from simple hexagons in a slow, continuous transition process. A third type of structure (honeycombs) forms from either white-eye patterns or hexagons. This transition occurs rapidly along propagating fronts. Two-dimensional Fourier analyses reveal that the complex patterns have a simple structure and that the wave vectors of the initial hexagons are conserved in all transitions. Quantitative data on surface undulations of the gel are presented. The surface structure resembles the structure of the observed methylene blue patterns. A schematic phase diagram is presented that characterizes the pattern geometry in terms of reaction time and initial sulfide concentration.

## Introduction

The polyacrylamide–methylene blue–oxygen (PA–MBO) reaction shows self-organization that gives rise to various patterns such as hexagons, stripes, and zigzag structures.<sup>1,2</sup> The question whether these patterns arise from convection phenomena during the gelation of the system or from a Turing-like chemical instability<sup>3–6</sup> is under discussion in the current literature.<sup>7–9</sup> Several findings support the hypothesis of a Turing-like instability: (a) experiments reveal that the response of the patterns to externally applied electric fields and light perturbations is in agreement with numerical results obtained from reaction–diffusion calculations;<sup>2,10</sup> (b) qualitative experimental results indicate that the patterns form several minutes after gelation;<sup>1</sup> (c) as shown in numerical simulations, the reaction mechanism of the MBO system has a structure that is capable of supporting Turing patterns.<sup>11</sup> In this context it has been proposed that molecular oxygen and hydrogen sulfide radicals play the role of inhibitors, while MB<sup>+</sup> acts as an activator. Recently, however, Kurin-Csörgei et al.<sup>7</sup> and Orbán et al.<sup>8</sup> reported the formation of similar patterns during the polymerization of acrylamide in the presence of sulfide ions. They concluded that methylene blue is not an essential species for the formation of patterns and that the patterns arise from Rayleigh–Bénard or Marangoni instabilities. In this scenario, convection rolls or cells are inducing local variations in the oxygen concentration, which subsequently gives rise to a nonuniform polymerization and a nonuniform swelling of the gel. Münster has recently questioned certain aspects of the study by Kurin-Csörgei et al.<sup>9</sup> In particular, it is unclear why Orbán et al.<sup>8</sup> found no or little dependence of the pattern wavelength (typically 2–3 mm) on the thickness of the system.

In this paper complex chevron and honeycomb patterns are described and analyzed, which are expected neither for typical reaction–diffusion media nor for convection systems. Additional data on white-eye patterns are presented. These complex patterns typically arise from simple hexagons in the complete PA–MBO

medium. The relevance of the presented results for the ongoing discussion on the nature of patterns in the PA–MBO reaction in general is discussed.

## Experimental Section

The MBO reaction is the methylene blue-catalyzed oxidation of HS<sup>−</sup> by oxygen in basic aqueous solution.<sup>12–14</sup> Methylene blue (MB) exists in three forms: the blue MB<sup>+</sup> ion, the colorless MBH, and the unstable MB<sup>•</sup> radical. The system is semiclosed, since the reactant oxygen is supplied from the air, while sulfide is continuously consumed. For a detailed discussion of the reaction mechanism in the context of chemical oscillations, see ref 13. Following the preparation of Watzl and Münster, we used the complete PA–MBO system and recrystallized sulfide.<sup>1</sup> However, NaOH was added to further increase the pH of the system and the polymerized gel was covered neither by water nor by a methylene solution. Additional experiments revealed no qualitative changes if the gel was covered with a thin layer of water. All experiments were carried out at room temperature. The blue patterns on a colorless background can be seen with the naked eye and were recorded by two-dimensional spectrophotometry for quantitative analyses.

Preparation of the system: 0.24 mL of *N,N'*-methylenebis(acrylamide) (2 g/100 mL of H<sub>2</sub>O), 0.13 mL of NaOH (0.5 M), and 0.25 mL of triethanolamine (30 g/100 mL of H<sub>2</sub>O) are added to 3.17 mL of acrylamide (20 g/100 mL of H<sub>2</sub>O). A mixture of 0.29 mL of methylene blue (0.318 g/100 mL of H<sub>2</sub>O), 0.5–0.65 mL of sulfide (3.902 g of Na<sub>2</sub>S/100 mL of H<sub>2</sub>O), and 0.87 mL of sulfite solution (Na<sub>2</sub>SO<sub>3</sub>; 0.252 g/100 mL of H<sub>2</sub>O) is added. Before starting the polymerization with 0.13 mL of ammonium persulfate (5 g/25 mL of H<sub>2</sub>O), double-distilled water is added to reach a final volume of 7.4 mL. Sodium sulfide was purified by refluxing commercially available Na<sub>2</sub>S with Cu powder in ethanol under a nitrogen atmosphere for 1 h.

A Petri dish (diameter: 7.0 cm) serves as the container of the PA–MBO reaction medium. The intensity of the applied observation light is an important parameter, since the reaction system is photosensitive. The light intensity was kept constant at 30 W/m<sup>2</sup>.

\* To whom correspondence should be addressed.

† Florida State University.

‡ Otto-von-Guericke-Universität Magdeburg.

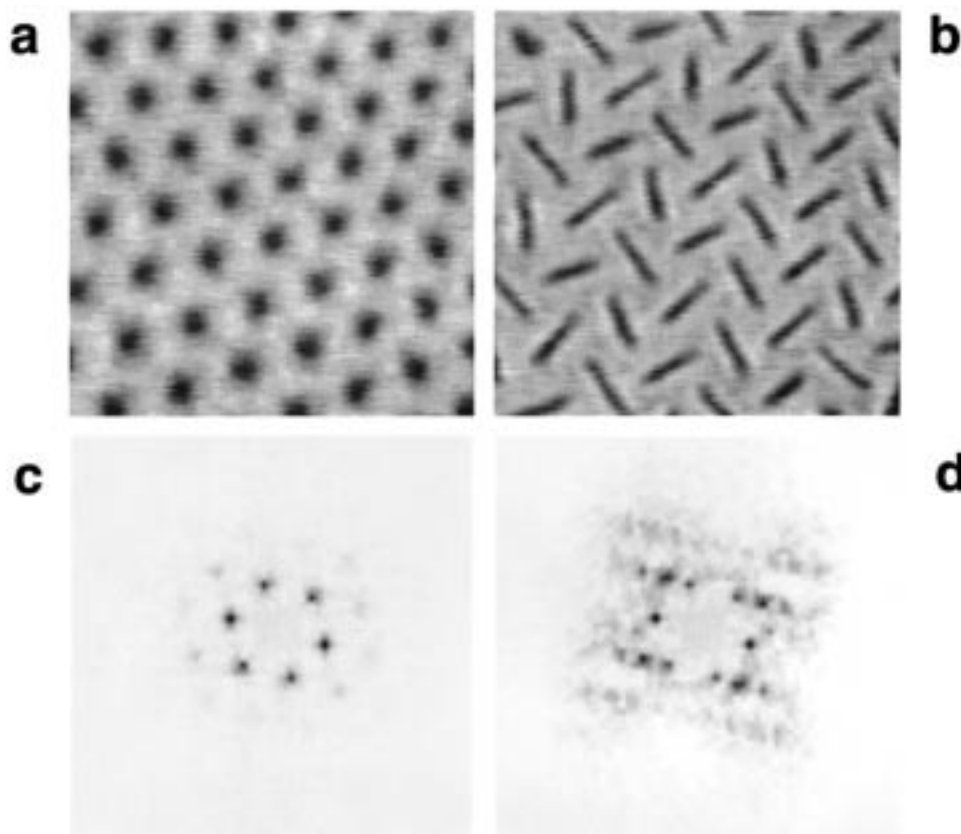


**Figure 1.** Transition from a hexagonal Turing pattern to a chevron-shaped concentration structure (a, b). Bright and dark regions correspond to areas with low and high  $\text{MB}^+$  concentration, respectively. Time between snapshots: 14 min. Image area:  $1.4 \times 1.4 \text{ cm}^2$ . (c) and (d) show the two-dimensional Fourier transforms of the images (a) and (b), revealing the occurrence of additional wave vectors (corresponding to four new spots in (d)) during this secondary bifurcation.

Under certain experimental conditions (e.g., strongly increased pH) a purple/pink precipitate was formed in the gelling PA–MBO system. This effect, however, was not observed for the concentration range specified above. A possible explanation for this precipitate is the formation of methylene azure B (trimethylthionine) or a closely related compound. Bergmann and O’Konski reported the formation of this compound from methylene blue via a demethylation reaction in a spectroscopic study of the methylene blue dimer.<sup>15</sup> The methylene blue dimer itself has been subject to various studies, which indicate that the structure of the dimer is “sandwich”-like.<sup>15,16</sup> The absorption maximum of the dimer is found at 605 nm (for the monomer: 664 nm). This dimer is most likely the species observed in thin gel sheets of the PA–MBO system by Watzl and Münster.<sup>1</sup> We want to reemphasize that the results presented in this Article are obtained from experiments that showed no signs of precipitation.

## Results

In the PA–MBO reaction, patterns arise approximately 10 min after preparation and have a wavelength of about 2–3 mm. In the course of the reaction we observed a transition from hexagonal patterns (Figure 1a) to a chevron-shaped structure (Figure 1b). The time interval between (a) and (b) is 14 min. The chevrons consist of parallel columns of needlelike regions of high  $\text{MB}^+$  concentration. Within a given column the orientation of the needles is typically the same, but quite different for the neighboring columns. A similar pattern has been recently reported by Kurin-Csörgei et al.<sup>7</sup>

To obtain a better understanding of the chevron pattern, two-dimensional Fourier transforms were calculated. The classic

hexagons (a) give rise to six main peaks in the corresponding Fourier space (c), thus, indicating that the pattern is mainly formed by the superposition of three arrays of stripes rotated by  $60^\circ$  with respect to each other. The Fourier transform (d) is obtained from snapshot (b) and shows that the original hexagonal pattern is still present after the transition to chevrons. However, four additional main peaks arise, which are located at the corners of a rectangle circumscribing the six original Fourier signals. This scenario is reminiscent of the zigzag instability of simple stripe patterns, which results in the formation of undulated stripes. The pure zigzag instability has been reported for several systems including the chlorite–iodide–malonic acid (CIMA) reaction<sup>17</sup> and electroconvection of liquid crystals.<sup>18</sup> In Fourier space it corresponds to the creation of four additional peaks quite similar to the case of the presented chevrons. In this context, the observed chevrons can be understood as a superposition of two arrays of straight stripe patterns with one array of zigzagging stripes.

In addition to the transition from hexagons to chevrons, one observes other phenomena that lead to structures of intriguing complexity. Figure 2a shows a snapshot of the MBO system with a concentration pattern that consists (in the left half) of small rings of high  $\text{MB}^+$  concentration with each ring located on a hexagonal lattice. This white-eye pattern develops from ordinary hexagons (compare, Figure 1a) that lose their dynamic stability in the course of the reaction. In this process each initial spot transforms into one ring without any significant change in location. Fourier analyses identify the white-eye pattern as a superposition of two hexagonal patterns, having a relative orientation of  $30^\circ$  and a wavelength ratio of about  $\sqrt{3}$ . This result suggests that the short wavelength lattice is a spatial

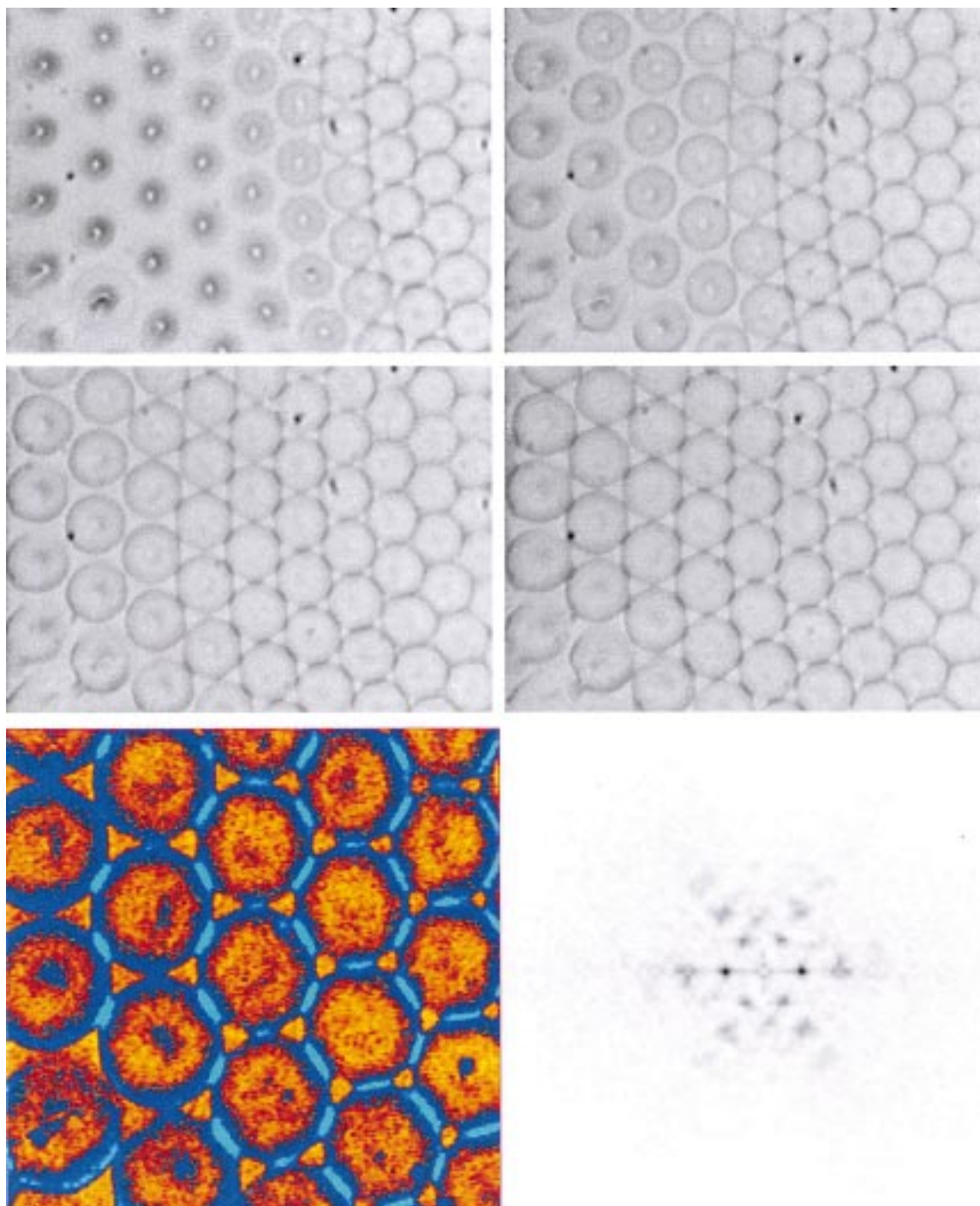


**Figure 2.** (a–d) Sequence of snapshots showing the transition from white-eye patterns (left-hand side of (a)) to honeycombs. The transition occurs along a propagating front. The resulting honeycomb pattern is shown as a pseudocolor representation (e), where orange and blue correspond to bright and dark regions, respectively. The two-dimensional Fourier transform of the honeycomb pattern is given in (f). Time between snapshots: 4 min (a, b), 3 min (b, c), 4 min (c, d). Image area:  $23 \times 16 \text{ mm}^2$ .

harmonic of the initial hexagonal pattern. It should be noted that similar concentration patterns were recently reported by Ouyang et al. for the CIMA reaction<sup>17</sup> and by Borckmans et al. in numerical simulations using the Brusselator model.<sup>19</sup>

In our preparation of the MBO reaction, the pattern shown in Figure 2a undergoes an additional bifurcation. About 20–40 min after the appearance of white eyes a fast transition occurs along a front propagating through the system. Figures 2a–c show typical snapshots of this transition with the front propagating from the right to the left. In the wake of the front an unexpected pattern of high complexity appears (see pseudocolor representation in Figure 2e), which will be referred to as the

honeycomb pattern. We found that such transition fronts typically nucleate from the physical boundary of the system or, less often, from regions with penta–hepta defects and grain boundaries. Notice that neither the transition from hexagons to white eyes nor to chevrons showed front properties. Also, the locations of the honeycomb cells do not always coincide with the locations of the initial rings. This leads typically to a decreased number of defects in the wake of the transition front.

Two-dimensional Fourier spectra of honeycomb patterns have a surprisingly simple structure (Figure 2f). The six peaks in the Fourier transform of the original hexagonal pattern are described by pronounced wave vectors at  $k_1$ ,  $k_2$ , and  $k_3$  and their

corresponding negative vectors. After the transition to white eyes, one observes the appearance of the spatial harmonics  $k_1 + k_2$ ,  $k_2 + k_3$ , and  $k_3 + k_1$ . These modes virtually disappear during the transition to honeycomb patterns and are replaced by the wave vectors  $2k_i$  and  $3k_i$  ( $i = 1, 2, 3$ ) and higher multiples of low intensity. The phases of  $nk_i$  were found to alternate between 0 and  $\pi$  for successive values of  $n$ . Consequently, honeycomb patterns can be described as a superposition of three hexagonal patterns with identical orientation, where the pattern with the largest wavelength corresponds to white spots (low  $[\text{MB}^+]$ ) on a black background (high  $[\text{MB}^+]$ ). Notice, that the wavelength and main orientation of the original hexagons (dark spots on bright background) is conserved in both transitions, but its phase changes in the transition from white eyes to honeycombs.

The change from hexagons to chevrons is slow compared to the transition from white eyes to honeycombs. A quantitative measure for this observation is the correlation  $c(t)$  between an initial image of the pattern and subsequent images of the same area:

$$c(t) \propto \sum_{x,y} (I_{x,y}^0 - \bar{I}^0) (I_{x,y}(t) - \bar{I}(t)) \quad (1)$$

where  $I_{x,y}^0$  and  $I_{x,y}(t)$  denote the intensity (i.e., gray levels) at the pixel site  $x, y$  of the initial and subsequent images, respectively. The variables  $\bar{I}^0$  and  $\bar{I}(t)$  are the mean intensity values of the corresponding images. Figure 3 shows the temporal evolution of this correlation for the transition to honeycombs (a) and the transition to chevrons (b). Figure 3a reveals that the hexagonal pattern does not change significantly during the first 10 min of the analyzed sequence. After approximately 11 min, the transition front passes through the observation area and induces a sudden decrease in the correlation. This decrease corresponds to the formation of honeycombs and a certain restructuring of the main lattice that also wipes out most of the defects. The sudden change is followed by a slow relaxation phase ( $t = 13\text{--}25$  min) that leads the chemical pattern into a new quasi-stationary state.

In the case of the transition from hexagons to chevrons (Figure 3b), the correlation function  $c(t)$  shows slow changes that correspond to the deformation of the original dots into needlelike segments (compare, Figure 1a,b). In most experiments the correlation was found to decrease monotonically. The asymptotic correlation value was typically  $0.6 \pm 0.1$ . However, we also found that the chevron needles can shrink again, thus, reestablishing more circular structures. A typical example for this phenomenon is shown in Figure 3b: The correlation decreases only during the first 17 min. At this time the needles have reached their maximal elongation. This phase is followed by the partial recovery of the original structure. However, the asymptotic pattern does not fully reach the circular dot geometry of the initial hexagons. Notice that the small decrease in the correlation between frames 0 and 1 ( $\Delta c \approx 0.05$ ) in Figure 3a,b is mainly caused by experimental noise.

The mean intensity of the images was obtained by averaging over the gray levels of all pixel sites and is also shown in Figure 3. The general increase of intensity is typical for the PA–MBO system and can be understood as a continuous reduction of  $\text{MB}^+$  ions to the colorless MBH. As can be seen clearly in Figure 3a, the slope of the intensity curve decreases significantly after the pattern has completed its transition ( $t \approx 12$  min).

The appearance of the patterns and the higher instabilities described above strongly depend on the initial concentration of  $\text{Na}_2\text{S}$ , and they occur at certain stages of the evolving reaction

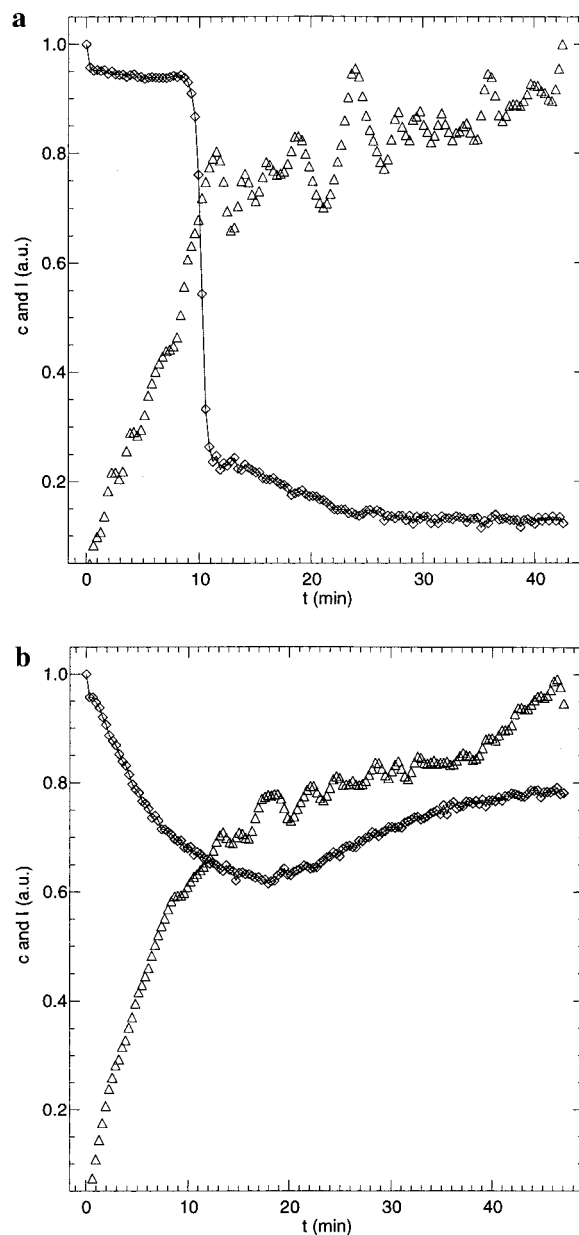


**Figure 3.** Analysis of the transition from a white-eye to a honeycomb pattern (a) and from hexagons to chevrons (b). The plots show the picture-averaged intensity  $I$  (triangles) and the cross-correlation  $c$  between different snapshots of the evolving pattern (diamonds) as a function of time. The cross-correlation was calculated according to eq 1 and characterizes the similarity between the first image of the sequence ( $t = 0$ ) and subsequent images. The analyzed image areas for (a) and (b) were  $3 \text{ cm}^2$ .

system. Figure 4 summarizes the results of numerous experiments in terms of a diagram that assigns a specific type of pattern to a characteristic reaction time and initial  $\text{Na}_2\text{S}$  concentration. Shortly after the onset of pattern formation, one observes only simple hexagons and stripes. For  $[\text{Na}_2\text{S}]_0 = 30\text{--}45$  mM the hexagons lose their stability after about 30 min, giving way to honeycombs. White-eye patterns can exist as an intermediate state. At higher  $\text{Na}_2\text{S}$  concentration, none of these patterns is found and the system continuously evolves to chevrons. In the phase-space of Figure 4 these chevrons are located close to the ordinary zigzag patterns (no photograph shown).

The concentration patterns described so far are closely related to local volume changes<sup>20</sup> of the polyacrylamide gel matrix. Nearly synchronously with the onset of pattern formation,

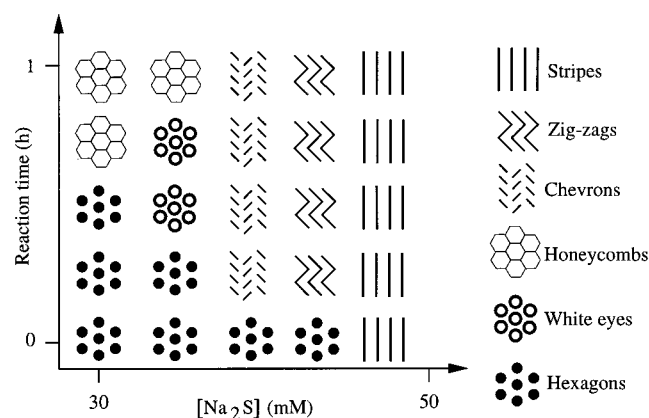


**Figure 4.** Schematic phase diagram summarizing different regions of pattern existence with respect to the initial sulfide concentration and the elapsed reaction time. The symbols representing different patterns are explained in the column on the right-hand side of the figure.

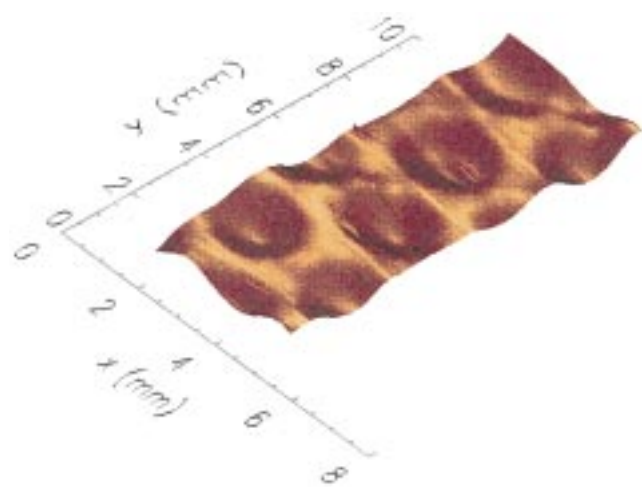


**Figure 5.** Surface profile of a dried polyacrylamide-MBO gel system. The hexagonal symmetry of the original Turing pattern is conserved in the surface structure. The dark valleys correspond to the locations of blue spots in the initial reaction system and have minima that are typically  $4 \mu\text{m}$  below the main surface. Gels were dried at room temperature for about 24 h. Scanned gel surface:  $3.75 \times 10.0 \text{ mm}^2$ .

changes in the surface of the gel occur that correlate with the emerging structures. These changes due to swelling and/or shrinking of the gel can be easily seen with the naked eye. Our experiments revealed that the resulting surface undulations remain present even in the completely dried-out polymer network. Quantitative data were obtained by using a Tencor P-10 Surface Profiler. Figure 5 shows a typical surface profile for an area of  $1.0 \times 0.375 \text{ cm}^2$ . In the dry film the maximal height differences amount to  $4 \mu\text{m}$  and the relative locations of the valleys yield a wavelength of about 2–3 mm. The locations of surface valleys correspond to regions that showed high concentrations of  $\text{MB}^+$ . The hexagonal symmetry as well as the wavelength are in good agreement with the main features of the initial patterns. The details of structures as realized in chevrons, white-eye, or honeycomb patterns seem to have typically no manifestation in the gel surface. Gap-like valleys, however, were occasionally observed for chevrons in systems with an increased concentration of bis(acrylamide).

## Conclusions

The semiclosed polyacrylamide-MBO system was shown to reveal at least three secondary transitions of the initial

hexagonal patterns, giving rise to chevron, white-eye, and honeycomb patterns. Despite extensive theoretical studies,<sup>18</sup> these patterns have not been predicted in the past, possibly because pattern formation in this system is linked to mechanical and/or chemical changes of the polyacrylamide network that are not considered in the classical reaction-diffusion approach. The dynamics of the transition from white-eye patterns to honeycombs differs significantly from that of the change from hexagons to chevrons. Up to now it is unclear what mechanisms induce this strikingly different behavior. The Fourier spectra of the observed patterns, however, are fairly simple and should provide a suitable basis for future comparison with theoretical analyses.

A remarkable finding of this study is that the hexagonal symmetry of the patterns formed during the early stages of the reaction is conserved in all subsequent structures. This appears to be a useful hint toward a better understanding of chevron, honeycomb, and white-eye patterns: Structural and mechanical changes of the gel matrix are a likely candidate for explaining this surprising memory effect of the PA-MBO system.

The fundamental questions whether the initial hexagonal patterns arise primarily from hydrodynamic or reaction-diffusion processes remain unanswered. The presented results, however, emphasize that pattern formation in this interesting system cannot be explained on the basis of hydrodynamic considerations alone, since the observed transitions to patterns of higher complexity occur after gelation and after formation of the hexagons.

**Acknowledgment.** We thank A. Münster for discussions and the Mikrostrukturzentrum, Otto-von-Guericke-Universität, Magdeburg for providing facilities.

## References and Notes

- Watzl, M.; Münster, A. F. *Chem. Phys. Lett.* **1995**, *242*, 273.
- Münster, A. F.; Watzl, M.; Schneider, F. W. *Phys. Scripta* **1996**, *T67*, 58.
- Turing, A. M. *Philos. Trans. R. Soc. London* **1952**, *B237*, 37.
- Castets, V.; Dulos, E.; Boissonade, J.; De Kepper, P. *Phys. Rev. Lett.* **1990**, *64*, 2953.
- Ouyang, Q.; Swinney, H. L. *Nature* **1991**, *352*, 610.
- Lengyel, I.; Kádár, S.; Epstein, I. R. *Science* **1993**, *259*, 493.
- Kurin-Csörgei, K.; Orbán, M.; Zhabotinsky, A. M.; Epstein, I. R. *Chem. Phys. Lett.* **1998**, *295*, 70.
- Orbán, M.; Kurin-Csörgei, K.; Zhabotinsky, A. M.; Epstein, I. R. *J. Phys. Chem. B* **1999**, *103*, 36.
- Münster, A. F. *Chem. Phys. Lett.*, in press.
- Watzl, M.; Münster, A. F. *J. Phys. Chem.* **1998**, *A102*, 2540.
- Eiswirth, M.; Münster, A. F. Manuscript in preparation.
- Burger, M.; Field, R. J. *Nature* **1984**, *307*, 720.
- Resch, P.; Field, R. J.; Schneider, F. W. *J. Phys. Chem.* **1989**, *93*, 2783.
- Zhang, Y.-X.; Field, R. J. *J. Phys. Chem.* **1991**, *95*, 723.
- Bergmann, K.; O'Konski, C. T. *J. Phys. Chem.* **1963**, *67*, 2169.
- Alperovich, L. I. *J. Struct. Chem.* **1994**, *35*, 43.
- Ouyang, Q.; Swinney, H. L. In *Chemical Waves and Patterns*; Kapral, R., Showalter, K., Eds.; Kluwer Academic Press: Dordrecht, The Netherlands, 1995.
- Kai, S.; Zimmermann, W. *Prog. Theor. Phys. Suppl.* **1989**, *99*, 458.
- Borckmans, P.; Dewel, G.; De Wit, A.; Walgraef, D. In *Chemical Waves and Patterns*; Kapral, R., Showalter, K., Eds.; Kluwer Academic Press: Dordrecht, The Netherlands, 1995.
- Li, Y.; Tanaka, T. *Annu. Rev. Mater. Sci.* **1992**, *22*, 243.